UC San Diego

UC San Diego Previously Published Works

Title

Cell of origin affects tumour development and phenotype in pancreatic ductal adenocarcinoma.

Permalink

https://escholarship.org/uc/item/55v6h52w

Journal

Gut, 68(3)

Authors

Lee, Alex

Dubois, Claire

Sarai, Karnjit

et al.

Publication Date

2019-03-01

DOI

10.1136/gutjnl-2017-314426

Peer reviewed

eScholarship.org Powered by the California Digital Library
University of California

Author Manuscript

Author Manuscript

Author Manuscript

Author Manuscript

HHS Public Access

Author manuscript

Gut. Author manuscript; available in PMC 2024 November 01.

Published in final edited form as:

Gut. 2019 March ; 68(3): 487–498. doi:10.1136/gutjnl-2017-314426.

Cell of origin affects tumor development and phenotype in pancreatic ductal adenocarcinoma

Alex Y.L. Lee[1], **Claire L. Dubois**[2], **Karnjit Sarai**[1], **Soheila Zarei**[1], **David F. Schaeffer**[3], **Maike Sander**[2], **Janel L. Kopp**[1,†]

[1]Department of Cellular and Physiological Sciences, University of British Columbia, Vancouver, British Columbia V6T 1Z3

[2]Departments of Pediatrics and Cellular & Molecular Medicine, University of California, San Diego, La Jolla, CA 92093-0695

[3]Department of Pathology and Laboratory Medicine, The University of British Columbia, Vancouver, British Columbia, Canada V6T 1Z3

Abstract

Objective: Pancreatic ductal adenocarcinoma (PDAC) is a highly aggressive tumor thought to arise from ductal cells via pancreatic intraepithelial neoplasia precursor lesions (PanINs). Modeling of different genetic events in mice suggests both ductal and acinar cells can give rise to PDAC. However, the impact of cellular context alone on tumor development and phenotype is unknown.

Design: We examined the contribution of cellular origin to PDAC development by inducing PDAC-associated mutations, $Kras^{G12D}$ expression and *Trp53* loss, specifically in ductal cells (*Sox9CreER;*$Kras^{LSL\text{-}G12D}$*;*$Trp53^{flox/flox}$ ("*Duct:*KP^{cKO}")) or acinar cells (*Ptf1a*^{CreER}*;*$Kras^{LSL\text{-}G12D}$*;*$Trp53^{flox/flox}$ ("*Acinar:*KP^{cKO}")) in mice. We then performed a thorough analysis of the resulting histopathological changes.

Results: Both mouse models developed PDAC, but *Duct:*KP^{cKO} mice developed PDAC earlier than *Acinar:*KP^{cKO} mice. Tumor development was more rapid and associated with high-grade murine PanIN (mPanIN) lesions in *Duct:*KP^{cKO} mice. In contrast, *Acinar:*KP^{cKO} mice exhibited wide-spread metaplasia and low-grade, as well as high-grade mPanINs with delayed progression to PDAC. Acinar-cell-derived tumors also had a higher-prevalence of mucinous glandular features reminiscent of early mPanIN lesions.

Conclusion: These findings indicate that ductal cells are primed to form *carcinoma in situ* that become invasive PDAC in the presence of oncogenic Kras and *Trp53* deletion, while acinar cells with the same mutations appear to require a prolonged period of transition or reprogramming to initiate PDAC. Our findings illustrate that PDAC can develop in multiple ways and the cellular

[†]Corresponding author: Janel Kopp, 2350 Health Sciences Mall, Vancouver, BC Canada V6T 1Z3, janelk@mail.ubc.ca, Fax: 604-822-2316.

Author Contributions A.L., C.L.D, and J.L.K acquired, analyzed, and interpreted the experiments and performed mouse husbandry; A.L. and J.L.K wrote the manuscript; D.F.S. provided advice on pathological classification of the tissue samples and critically reviewed the manuscript; M.S. and J.L.K obtained funding, supervised the study, and critically reviewed the manuscript; J.L.K conceived of the study concept and design. All authors reviewed and approved of the submitted manuscript.

Author Manuscript Author Manuscript Author Manuscript Author Manuscript

context in which mutations are acquired has significant impact on precursor lesion initiation, disease progression, and tumor phenotype.

Keywords

tumor development; pancreatic cancer; tumor heterogeneity; lineage tracing

INTRODUCTION

Pancreatic ductal adenocarcinoma (PDAC) is characterized as a mass of haphazard ductules arranged in a desmoplastic stroma. The histological similarity of these ductules and associated precancerous lesions, called pancreatic intraepithelial neoplasia (PanIN), to pancreatic ductal cells suggested a lineage relationship and led to the development of tumor progression models that featured the normal ductal cell as the cellular origin of PDAC.[1] In these models, oncogenic Kras, one of the most common mutations in PDAC, is proposed to initiate low-grade PanIN from ductal cells. These lesions then acquire additional mutations, such as p16 or p53 loss, before becoming high-grade PanIN and invasive PDAC.[1] However, acinar cells were found in early metaplastic ductules[2 3] and lineage traced into a ductal-cell-like fate[4 5] suggesting that acinar cells could act as a cellular origin for PDAC. Indeed, multiple studies have shown that oncogenic Kras expression in murine acinar cells triggers widespread ductal metaplasia, murine PanIN (mPanIN), as well as PDAC.[6–11] In contrast, oncogenic Kras expression in ductal cells induces only a small number of low-grade mPanIN.[10 12] In sum, experimental evidence predominantly supports the potential of acinar cells to initiate mPanIN and PDAC; however, the data regarding ductal cell potential is limited.

Although ductal cells can contribute to mPanINs,[10 12] whether these ductal-cell-derived lesions progress in the same manner as acinar-cell-derived mPanIN, or whether they are viable cell of origin for PDAC is unclear. Recent studies have started to directly compare the potential of acinar and ductal cells to initiate PDAC.[6 13 14] Using mouse models, these studies show that both ductal and acinar cells have the potential to form PDAC.[6 13 14] However, the acinar- or ductal-cell-derived tumors were formed under different treatment conditions or with different genetic mutations,[6 13 14] therefore, it is remains unclear whether the differences in tumor development or phenotype observed were a result of the treatment conditions, mutation combination, or cellular origin. Thus, studies to specifically examine the cell-of-origin-specific effects are needed and could highlight the initiating cell as a source of PDAC heterogeneity.

To isolate the effect of cell of origin alone on PDAC initiation, development, and phenotype, we used CreER-inducible mouse models to make the same genetic changes, expression of oncogenic $Kras^{G12D}$ and ablation *Trp53* (occurring in ~92% and ~27% of human PDAC samples, respectively[15]), in ductal or acinar cells. We found that cell of origin alone can impact the initiation and phenotype of PDAC.

Author Manuscript Author Manuscript Author Manuscript Author Manuscript

MATERIALS AND METHODS

Mice

All described animal experiments were approved by the University of British Columbia and University of California, San Diego Animal Care and Use Committees. The sources and phenotypes for the mouse strains, as well as details of genotyping and endpoint monitoring strategies are provided as online Supplemental Information. Recombination was induced by three subcutaneous injections of tamoxifen in corn oil (20mg/ml) over five days at 0.125g tamoxifen/g body mass.

Histology, Immunohistochemical and Immunofluorescence Analyses

Paraffin-embedded or frozen sections were prepared and stained using hematoxylin and eosin, Alcian blue, immunohistochemical or immunofluorescence stains as described previously.[10 16–18] Histological and morphometric analyses were conducted by A.L. and J.L.K. independently and verified by D.F.S. (gastrointestinal pathologist). Detailed descriptions of staining and morphological assessment methods, as well as the antibodies used, are provided as online Supplemental Information.

Statistical analysis

Normal distribution, F-test of variance, and parametric and non-parametric P-values were calculated in GraphPad Prism or Excel or statistical programming language R, version 3.4.1 (R Core Development Team, 2017) software. Graphpad Prism was used to calculate the mean and standard error of the mean (SEM). We performed a linear regression using the statistical programming language R, version 3.4.1 (R Core Development Team, 2017) to test if there was a significant ($p<0.05$) relationship between time post tamoxifen injection and tumor number or size.

RESULTS

Loss of *Trp53* and activation of Kras in ductal compared to acinar cells shortens survival in mice

To determine how cellular origin affects the initiation and progression of PDAC, we generated mouse models in which a shared set of PDAC-associated mutations[15 19 20] in *Kras* and *Trp53* were induced in a cell-type-specific manner. Specifically, we used the Cre-dependent $Kras^{LSL\text{-}G12D}$ [21] and $Trp53^{flox}$ conditional alleles[22]) to activate Kras and ablate p53 expression, respectively. To trace the fate of recombined cells, we also included a Cre-dependent $R26R^{YFP}$ reporter allele.[23] Finally, Cre-mediated recombination was induced in adult ductal or acinar cells using the tamoxifen-inducible *Sox9CreER* transgene[18 24] or $Ptf1a^{CreER}$ allele,[25] respectively. By combining all of these alleles through cross breeding and injecting the offspring with tamoxifen at three to four weeks of age (Figure 1A–B), we generated $Sox9CreER;Kras^{LSL\text{-}G12D};Trp53^{flox/flox};R26R^{YFP}$ (hereafter referred to as $Duct{:}KP^{cKO}$) and $Ptf1a^{CreER};Kras^{LSL\text{-}G12D};Trp53^{flox/flox};R26R^{YFP}$ (hereafter referred to as $Acinar{:}KP^{cKO}$) mice (Figure 1A). Mice injected with tamoxifen, but lacking the *Kras* oncogene were used as controls ($Sox9CreER;Trp53^{flox/flox};R26R^{YFP}$ or $Ptf1a^{CreER};Trp53^{flox/flox};R26R^{YFP}$ mice). Four weeks after tamoxifen injection, we observed

Author Manuscript Author Manuscript Author Manuscript Author Manuscript

highly efficient and specific labeling of $Sox9^+$ ductal or carboxypeptidase $A1^+$ ($Cpa1^+$) acinar cells in *Sox9CreER;Trp53*$^{flox/flox}$*;R26R*^{YFP} or *Ptf1a*^{CreER}*;Trp53*$^{flox/flox}$*;R26R*^{YFP} mice, respectively (Figure S1A–B). As previously reported,[24 25] little or no recombination of the *R26R*^{YFP} allele was observed in un-injected mice with the *Sox9CreER* or *Ptf1a*^{CreER} allele, respectively (Figure S1C).

To examine the effect of activating Kras and ablating *Trp53* on ductal and acinar cells, we injected a cohort of *Duct:KP*^{cKO} (n= 19) and *Acinar:KP*^{cKO} (n=9) mice with tamoxifen at three to four weeks of age and monitored the animals until their humane endpoint (Figure 1B). In addition to the pancreas, this *Sox9CreER* allele[24] is expressed in the oral mucosa, mammary gland, and lung. Therefore, eleven *Duct:KP*^{cKO} mice reached their humane endpoint due non-pancreatic masses, were censored from the PDAC-specific survival curve, and excluded from further analysis (Figure 1C). The remaining *Duct:KP*^{cKO} mice (n=8) reached their humane endpoint within 10–13 weeks post tamoxifen injection (Figure 1C). In contrast, *Acinar:KP*^{cKO} mice reached their humane endpoint at 15–23 weeks post tamoxifen injection (Figure 1C). Upon necropsy, we found pancreatic tumors (Figure 1D) in *Duct:KP*^{cKO} and *Acinar:KP*^{cKO} mice that blocked the bile duct resulting in jaundice, penetrated the small bowel, and/or induced large amounts of hemorrhagic or clear ascites fluid (Table 1). Control *Sox9CreER;Trp53*$^{flox/flox}$*;R26R*^{YFP} or *Ptf1a*^{CreER}*;Trp53*$^{flox/flox}$*;R26R*^{YFP} mice of similar or older ages were anatomically normal (Figure 1D and data not shown). Occasionally, local splenic, duodenal, or perineural invasion (7 of 8 *Duct:KP*^{cKO} mice and 5 of 8 *Acinar:KP*^{cKO} mice) was observed. Distant metastases to the peritoneal wall, diaphragm, and potentially liver were observed only in *Duct:KP*^{cKO} mice (6 of 8 *Duct:KP*^{cKO} mice)(Figure S1B–D and Table 1). However, the small liver adenocarcinomas could not be definitively distinguished as cholangiocarcinoma vs. metastatic PDAC, therefore the lineage of these liver lesions is uncertain. Together, these data suggested that loss of *Trp53* in $Kras^{G12D}$-expressing ductal or acinar cells induced PDAC. However,*Acinar:KP*^{cKO} mice had a median PDAC specific survival period that was approximately seven weeks longer than *Duct:KP*^{cKO} mice ($p< 0.0001$) and did not have any signs of distant metastases (Table 1), suggesting that cell of origin alone can affect tumor development and phenotype.

Cell of origin affects PDAC histology and timing

To determine whether differences in the survival outcomes of *Duct:KP*^{cKO} and *Acinar:KP*^{cKO} mice were due distinct tumour attributes, we extensively characterized the tumors in *Duct:KP*^{cKO} and *Acinar:KP*^{cKO} mice. Pancreata from both *Duct:KP*^{cKO} and *Acinar:KP*^{cKO} mice, but not controls, had solid tumor nodules, ranging from small, distinct nodes to complete displacement of the normal parenchyma by tumors (Figure 1D and Figure 2A, tumors outlined with white dashed line). Hematoxylin and eosin staining confirmed that these tumors were comprised of glandular structures arranged in a haphazard pattern (Figure 2B) consistent with PDAC. Further characterization by immunohistochemical staining demonstrated that tumors from both genotypes were ductal in nature (Cytokeratin 19^+, Figure 2C and Table 1; $Sox9^+$ and $Hnf1b^+$, Figure S2A) and arose from YFP^+ lineage traced cells (Figure 2C) that had recombined the *Kras*$^{LSL\text{-}KrasG12D}$ and *Trp53*^{flox} loci (Figure S2B) and lacked p53 expression (Figure S2C, arrowheads indicate

Author Manuscript Author Manuscript Author Manuscript Author Manuscript

p53^{+} stromal cells). Histologically, tumors from *Duct:KP^{cKO}* and *Acinar:KP^{cKO}* mice were predominantly comprised of moderately differentiated cells arranged in small glandular structures surrounded by collagen-rich stroma (Figure 2B and 2D and Figure S3). However, areas of well- and poorly-differentiated epithelium were also present (Figure S3A) that had higher and lower amounts of stroma, respectively (Figure S3B–C). Interestingly, a number of tumors from *Acinar:KP^{cKO}* mice, but rarely *Duct:KP^{cKO}* mice, were comprised of atypical glands with abundant supranuclear mucin resembling mPanIN lesions (denoted as “Mucinous-gland”) or larger atypical gland structures (denoted as “Large-gland”) (Figure 2D and Table 1). Although there were some differences in the histological appearance of *Duct:KP^{cKO}* and *Acinar:KP^{cKO}* tumors that correlated with the amount of stroma present in the tumor, on average, the amount of pancreatic area displaced by tumors was similar in *Duct:KP^{cKO}* and *Acinar:KP^{cKO}* mice at their respective endpoints (Figure 3). In addition, no difference in the size, number, or location of individual tumors was observed (Figure S4A–C). Altogether our thorough characterization of *Duct:KP^{cKO}* and *Acinar:KP^{cKO}* tumors suggested that there were some phenotypic differences in tumors arising from different cells types. However, the most striking observation made was that the tumor burden reached its peak earlier in *Duct:KP^{cKO}* compared to *Acinar:KP^{cKO}* mice (Figure 3). This suggests differences in the timing of tumor initiation from ductal and acinar cells may underlie the differences in survival of *Duct:KP^{cKO}* and *Acinar:KP^{cKO}* mice.

Tumors initiate earlier in *Duct:KP^{cKO}* compared to *Acinar:KP^{cKO}* mice

To study tumor initiation in *Duct:KP^{cKO}* and *Acinar:KP^{cKO}* mice, we examined pancreata from these mouse models at time points approximately at or before the earliest death observed in each model (Table 1). Specifically, we injected mice of both genotypes at three to four weeks of age with tamoxifen (n=4 per time point) and then collected and analyzed the size and number of tumors arising in *Duct:KP^{cKO}* and *Acinar:KP^{cKO}* pancreata between 2 to 8 or 4 to 16 weeks post injection, respectively (Figure 4A). At four weeks post tamoxifen injection, we found that two *Duct:KP^{cKO}* mice already had a microscopic tumor less than 1mm in size (Figure 4B–C, Figure S5A and S5C, tumors denoted by arrowheads). Subsequently, the number of tumors in *Duct:KP^{cKO}* mice significantly increased with respect to time ($p<0.01$). The size of the tumors did not significantly with time ($p=0.3672$), likely because the continual generation small tumors reduced the overall average (Figure 4B–C and Figure S5A). In contrast, no tumors were observed in *Acinar:KP^{cKO}* mice until eight weeks post tamoxifen injection (Figure 4B–C, Figure S5B and S5D, tumors denoted by arrowheads) and the increase in the number of tumors after eight weeks did not correlate with time (Figure 4B, $p=0.2632$). Once tumors formed in *Acinar:KP^{cKO}* mice, though, their size significantly increased with time (Figure 4C, $p<0.001$) suggesting that growth was a more dominant mechanism than tumor initiation in the acinar-cell-derived mouse model. Taken together, these data suggest that differences in the time of PDAC initiation resulted in the distinct survival intervals of *Duct:KP^{cKO}* and *Acinar:KP^{cKO}* mice. In support of this, the four week delay in tumor initiation observed in the *Acinar:KP^{cKO}* mouse model approximately matched the difference in time (34 days) between the first animals of each model succumbing to the disease (Figure 1C and Table 1).

Author Manuscript Author Manuscript Author Manuscript Author Manuscript

Duct:KP^{cKO} mice develop only high-grade mPanINs, which progress to invasive PDAC faster than those from *Acinar:KP^{cKO}* mice

Since we observed earlier PDAC initiation from ductal compared to acinar cells, we next examined whether this was a result of differences in precursor lesion initiation and/or progression. To do this, we quantified the number and grade of mPanINs present per pancreatic section from *Duct:KP^{cKO}* and *Acinar:KP^{cKO}* pancreata harvested between 2 to 8 or 4 to 16 weeks post injection, respectively (Figure 4A). Consistent with previous studies showing that Kras^{G12D}-expressing acinar cells form abundant low-grade mPanINs,[7–11 16] at four weeks post injection, we found numerous low-grade mPanIN lesions in *Acinar:KP^{cKO}* pancreata and they increased in number over time (Figure 5A–B). We also found high-grade mPanIN in *Acinar:KP^{cKO}* mice beginning at four weeks post injection and the number increased to approximately twenty mPanIN3 lesions per section per mouse by 16 weeks post-injection (Figure 5B). This suggests that a progression from low- to high-grade mPanIN could occur from Kras^{G12D}-expressing acinar cells in the absence of *Trp53*. In contrast, we found a small number of mPanIN3, but no mPanIN1, lesions in *Duct:KP^{cKO}* mice at all time points analyzed (Figure 5A–B). Interestingly, the number of mPanIN3 lesions in *Duct:KP^{cKO}* and *Acinar:KP^{cKO}* mice were comparable at four weeks post injection (~one per section per mouse) (Figure 5B). However, *Duct:KP^{cKO}* mice already had small microtumors at this time point (Figure 4B–C), while *Acinar:KP^{cKO}* mice did not develop invasive lesions for another month (Figure 4B). Together these data suggest that the reduced survival time of *Duct:KP^{cKO}* compared to *Acinar:KP^{cKO}* mice may be due to the increased propensity of Kras^{G12D}-expressing ductal cells to induce mPanIN3 that convert to invasive PDAC in the absence of *Trp53*.

To ensure that the discrepancy in mPanIN3 progression was not due to differential recombination of the *Trp53^{flox}* allele in Kras^{G12D}-expressing acinar and ductal cells, we used p53 immunohistochemistry to examine p53 status in mPanIN from *Duct:KP^{cKO}* and *Acinar:KP^{cKO}* pancreata. Ductal- and acinar-cell-derived mPanIN3 were both uniformly p53-negative (Figure S6A) suggesting that these lesions arose from *Trp53*-ablated cells. Thus, the presence of p53 does not explain the delayed progression of acinar-cell-derived mPanIN3 to PDAC. In contrast to mPanIN3 lesions, p53 expression in the acinar-cell-derived low-grade mPanIN was more variable with some lesions completely lacking p53, and others expressing high levels of p53 (Figure S6B). Thus, the large parenchymal area displaced by abnormal duct-like lesions (approximate 30%)(Figure S6C) in some *Acinar:KP^{cKO}* pancreata is likely comprised of low-grade Kras^{G12D+}p53^{-} and Kras^{G12D+}p53^{+} lesions, while mPanIN3 and PDAC arise from Kras^{G12D+}p53^{-} cells.

To examine potential differences between acinar- and ductal-cell-derived mPanIN3, we examined whether cell death or proliferation might differ in these lesions. We found little to no cell death, as denoted by cleaved caspase 3 positivity, in the mPanIN3 lesions (Figure S6D) and the average percent of Ki67^{+} cells per mPanIN3 was similar between cellular origins (Figure 5C–D, p=0.09792). However, the variance in number of proliferating cells between the ductal and acinar cell model was significantly different (Figure 5D, F-test, p=0.01372). This suggests that there was more heterogeneity in the proliferative rate of

Author Manuscript Author Manuscript Author Manuscript Author Manuscript

acinar- compared to ductal-cell-derived mPanIN3 lesions, which could underlie some of the differences in mPanIN3 progression between cellular origins.

Acinar-cell-derived PDAC often retains molecular properties associated with low-grade mPanIN

Because mucinous low-grade mPanINs were more prevalent in *Acinar:KP^{cKO}* compared to *Duct:KP^{cKO}* mice (Figure 5B) and tumors derived from acinar cells tended to contain more highly mucinous-glands (Figure 2D and Table 1), we next asked whether tumors formed from acinar cells might retain a molecular "memory" of their transition through a low-grade mucinous mPanIN stage. To address this question, we examined whether acinar-cell-derived PDAC maintained characteristics typical of low-grade mPanINs, such as expression of acidic mucins or Mucin 5AC (Muc5AC).[26] We found that acinar-cell-derived tumors had moderate to strong levels of Alcian blue (acidic mucin stain) and Muc5AC staining that frequently, but not exclusively, correlated with histological areas containing mucinous glands (Figure 6A–C). Quantification of the percent total tumor area occupied by Alcian blue^{+} or Muc5AC^{+} glands in *Acinar:KP^{cKO}* and *Duct:KP^{cKO}* mice (n=8 for each genotype) illustrated that acinar-cell-derived tumors on average contained more acidic mucins and Muc5AC expression than ductal-cell-derived PDAC (Figure 6C–D, $p<0.001$ and $p<0.05$, respectively). Importantly, the Alcian blue and Muc5AC positivity was not restricted to tumors we previously characterized as "large-gland" or "mucinous-gland", but was found in a larger number of acinar-cell-derived PDAC. Altogether, our data showed that low-grade mPanIN characteristics and premalignant low-grade mPanINs are highly associated with acinar-, but not ductal-cell-derived PDAC. This suggests that the developmental route of acinar- and ductal-cell-derived tumors in mice can impact tumor histopathology, as well as the molecular phenotype.

Recent studies have described a number of different PDAC subtypes. To determine whether acinar- or ductal-cell-derived PDAC may be similar to these molecular subtypes, we performed immunohistochemistry for one of the markers associated with the "classical" PDAC subtype, Keratin 20 (CK20).[27] We found signal for this marker was very intense in the highly mucinous glands of acinar-cell-derived PDAC (Figure 6E). Quantification of CK20 signal in ductal- and acinar-cell-derived PDAC indicates that CK20 is significantly higher in acinar- compared to ductal-cell-derived tumors (Figure 6F). This suggests that at least some of the acinar-cell-derived tumors may be similar to the "classical" subtype of PDAC. However, a more comprehensive analysis of multiple markers is needed before cell of origin can be implicated as a source of heterogeneity in PDAC.

Discussion

Ductal cells are a cellular origin of mPanIN-associated PDAC

Our study demonstrates that Kras^{G12D}-expressing ductal cells quickly form high-grade mPanIN and convert to PDAC in the absence of *Trp53*. The absence of low-grade PanIN, which readily form from acinar cells,[8 10 11 16] in *Duct:KP^{cKO}* mice even though a small number of Cpa1^{+} cells are labeled by the *Sox9CreER* allele argues that acinar cells are not contributing to the tumorigenesis observed in *Duct:KP^{cKO}* mice. In addition, the absence of

Author Manuscript Author Manuscript Author Manuscript Author Manuscript

low-grade mPanIN in our study, as well as that of Bailey et al.,[6] suggests that ductal cells do not need to transition through a low-grade mPanIN stage to form PDAC in the absence of functional *Trp53*. Typically, only PanIN3 and PDAC are thought to possess mutations in *Trp53*.[28 29] Thus, the animal models in ours and Bailey et al.[6] studies may provide mutations sufficient for tumor formation and result in ductal cells bypassing the low-grade mPanIN stage. Importantly, these findings do not supersede previous observations that $Kras^{G12D}$-expressing ductal cells form low-grade mPanINs.[10 12] Although the tumorigenic potential of the ductal-cell-derived mPanINs were not examined in previous studies,[10 12] our subsequent studies demonstrated that loss of the tumor suppressor *Pten* alone (*Sox9CreER;Pten*$^{flox/flox}$ mice) in ductal cells could result in low-grade, as well as high-grade mPanIN that were associated with PDAC in the context of large duct metaplasia (Kopp et al, 2017 *in review*). In addition, combining oncogenic Kras expression with heterozygous loss of *Pten* in ductal cells (*Sox9CreER;Kras*$^{LSL\text{-}G12D}$*;Pten*$^{flox/+}$ mice) promoted mPanIN-associated PDAC induction (Kopp et al, 2017 *in review*). Although our studies suggest that ductal cells are capable of initiating tumorigenesis via the proposed PanIN progression model,[1] this is likely dependent on genetic context and PanINs may not always be necessary. Thus, the current PanIN progression model[1] may only capture a simplified picture of the way tumors develop and this model may need to be revised to incorporate the context of specific genetic mutations and distinct cells of origin.

Acinar-cell-derived tumorigenesis is delayed and more stochastic than ductal-cell-derived tumorigenesis

In contrast to *Duct:KP*^{cKO} mice, *Acinar:KP*^{cKO} mice develop the entire spectrum of low- to high-grade mPanIN lesions from $Kras^{G12D}$-expressing p53-negative cells. This suggests that acinar-cell-derived mPanINs might follow a progression model where low-grade mPanIN precede high-grade mPanIN.[1] Unlike ductal cells, acinar cells must change a large portion of their transcriptional program to become ductal-cell-like mPanIN and PDAC. Thus, it is possible that this acinar-to-ductal-cell-like transition slows the initiation of PDAC from most $Kras^{G12D}$-expressing, p53-deleted acinar cells and favors the accumulation of lesions at multiple stages of the acinar cell-to-PDAC progression scheme.[16] In support of this theory, we found 1) mPanIN lesions of all grades accumulate with time in *Acinar:KP*^{cKO} mice; 2) some acinar-cell-derived-PDAC had large areas of highly mucinous glands and maintained strong expression of low-grade mPanIN markers; and 3) the duration of time until *Acinar:KP*^{cKO} mice initiated tumors or reached their humane endpoint varied widely from mouse to mouse, but was very predictable for the *Duct:KP*^{cKO} mouse model. Altogether, these data suggest that acinar-cell-mediated tumorigenesis may be a halting or stochastic process requiring additional epigenetic or genetic events to occur for progression to PDAC. As a result of this randomized process of progression, we might expect that PDAC arising from acinar cells would be more heterogeneous. Consistent with this, we observed a greater number of histological phenotypes and variability in mucin and CK20 expression in acinar- vs. ductal-cell-derived PDAC. Thus, the process of acinar cell-to-PDAC transformation, at least in mice, is highly variable and results in more inter-tumoral heterogeneity.

Not only are acinar- and ductal-cell-derived PDAC associated with different grade of mPanIN, it appears that mPanIN3 derived from acinar cells are not equivalent to those from

Author Manuscript Author Manuscript Author Manuscript Author Manuscript

ductal cells. A number of possible brakes or checkpoints could underlie the differences in acinar- vs ductal-cell-derived tumorigenesis from mPanIN3. For example, previous studies have shown that the acinar-cell-differentiation program limits the number of acinar cells switching to the ductal-cell-like mPanIN fate in response to the Kras oncogene.[30–34] Moreover, removing $Kras^{G12D}$ reverts these mPanIN cells to the acinar cell fate.[35] Thus, the transcriptional or epigenetic status of the terminally differentiated acinar cell may persist for some time once they have converted to duct-like cells and potentially limit PDAC initiation. Although a similar transcriptional mechanism for the ductal cell fate has been proposed to limit induction of cystic precursor lesions from ductal cells,[36] the role of this program in ductal-cell-mediated mPanIN-PDAC is unknown.

Another potential cellular program known to limit acinar-cell-mediated mPanIN and PDAC formation is oncogene-induced senescence. Guerra and colleagues demonstrated that $Kras^{G12V}$ expression in acinar cells induces low-grade mPanIN lesions that become senescent or growth arrested.[37] Thus, induction of cell cycle arrest proteins, like p16, might be important for halting acinar-cell-derived tumorigenesis. In support of this we observed a greater variation in proliferation in acinar-cell-derived PanIN3 lesions compared to their ductal-cell-derived counterparts. This variation could be due to localized inflammation, that previous studies demonstrated reduced the growth-arrested phenotype in acinar-cell-derived mPanIN.[37] This suggests that increased inflammation due to pancreatitis could specifically decrease the latency of acinar-cell-derived tumorigenesis. The role of senescence in ductal-cell-mediated mPanIN formation and progression, however, is unclear and the growth arrest associated with $Kras^{G12D}$ expression may not occur in this cell type or it may be completely dependent upon p53.

Finally, the biggest difference between $Acinar{:}KP^{cKO}$ and $Duct{:}KP^{cKO}$ mice is the quicker transition of ductal-cell-derived mPanIN3, or ductal *carcinoma in situ*, into invasive lesions. Therefore, the increased propensity of cells within ductal-cell-derived mPanIN to invade the basement membrane and move into the stroma becoming PDAC could underlie the differences in mPanIN3 derived from different cell types. Consistent with a role for invasion in the difference between ductal- and acinar-cell-derived tumorigenesis, we observed metastases to the diaphragm and peritoneum in two $Duct{:}KP^{cKO}$ mice, but distant metastases were not present in $Acinar{:}KP^{cKO}$ mice. While these observations are based on a limited number of animals, the data supports the conclusion that ductal-cell-derived tumorigenesis is associated with a more invasive phenotype. Additional studies examining the differential expression of factors involved in cell-to-cell adhesion or the epithelial-to-mesenchymal transition could illuminate potential molecular mechanisms underlying this difference in invasiveness. In sum, future studies are needed to examine each of these specific candidate programs to gain mechanistic insight into why ductal-cell-derived mPanIN induce PDAC more rapidly than their acinar-cell-derived counterparts.

Impact of more than one cellular origin of PDAC on preclinical PDAC models

Many studies have characterized the specific effects of distinct genetic mutations on PDAC initiation and development, with the majority of studies using pan-pancreatic mouse models driven by combining the *Pdx1-Cre* or $Ptf1a^{Cre}$ alleles with the $Kras^{LSL\text{-}G12D}$ allele and

Author Manuscript Author Manuscript Author Manuscript Author Manuscript

conditional knockout alleles for the gene of interest.[38–41] This would result in both acinar and ductal cells expressing oncogenic Kras and losing expression of the gene of interest. In the case of *Trp53*, evidence from our study and that of Bailey et al.[6] would suggest that ductal and acinar cells respond differently to whether the activity of one or both alleles of *Trp53* is lost.[6] Specifically, Bailey et al.[6] found that heterozygous *Trp53R172H* mutations in $Kras^{G12D}$-expressing acinar, but not ductal cells induced PDAC. In contrast, we found homozygous disruption of *Trp53* in both $Kras^{G12D}$-expressing ductal and acinar cells induced PDAC, but acinar cells required more time for PDAC induction.[6] This suggests there may be cell-of-origin-specific effects at play in pan-pancreatic mouse models that have been previously unrecognized. For example, our data would predict that the first tumors observed in *Pdx1-Cre;*$Kras^{LSL\text{-}G12D/+}$*;*$Trp53^{flox/+}$ or *Pdx1-Cre;*$Kras^{LSL\text{-}G12D}$*;*$Trp53^{R172H/+}$ mice may be acinar-cell derived, however the initial tumors found in *Pdx1-Cre;*$Kras^{LSL\text{-}G12D/+}$*;*$Trp53^{flox/flox}$ or *Pdx1-Cre;*$Kras^{LSL\text{-}G12D}$*;*$Trp53^{R172H/R172H}$ mice could instead be ductal-cell derived due to faster carcinoma initiation from this cell type. It is possible that other confounding factors, such as any effect of the embryonic context, may complicate whether observations in our cell-type-specific mouse models could be simply extrapolated to embryonically-induced pancreatic cancer models. Nevertheless, it is clear from our studies and others[6 9 14] that even subtly changing the genetic context (homozygous vs heterozygous mutation) could dramatically change the PDAC cellular origin, and potentially tumor phenotype. Therefore, greater care should be taken to analyze genetic mutations in the context of the adult cell types from which PDAC likely arises.

Significance of more than one PDAC cell of origin

We have shown that cell of origin is an important factor to consider when using mouse models to study PDAC. It can affect tumor initiation and progression and may also affect the tumor phenotype. This raises that possibility that cell of origin may underlie the generation of interpatient tumor heterogeneity and differential clinical outcomes. Interestingly, one of the main phenotypes distinguishing acinar- and ductal-cell-mediated tumorigenesis appears to be the accumulation of low- and high-grade mPanIN lesions during acinar-cell-mediated tumorigenesis. Recent studies examining the number of PanIN lesions of different grades adjacent to resected tumors have found that patients can be separated into two general groups: those with the entire spectrum of PanIN lesions (PanIN1–3) and those with no PanIN3 and little or no PanIN1.[42–44] Interestingly, the latter patients have a significantly worse prognosis compared to those whom had a higher number of PanINs. Because PanINs that give rise to PDAC are likely obscured by the growing tumor, a larger number of PanINs present in the resection margin is likely the result of a field effect. In addition, $Kras^{G12D}$-expressing acinar cells are more susceptible to inflammation and more easily give rise to mPanIN. Therefore, the accumulation of PanINs in the resected margin may indicate that these patients have a predisposition for their acinar cells to induce tumors. However, those patients with very little evidence of a field effect may have been predisposed to form ductal-cell-derived PDAC that developed with very little impact on the rest of the pancreatic parenchyma. While our data suggests just one possibility to explain the aforementioned correlates, definitively connecting these clinical observations with our observations of tumorigenesis in mouse models will require generation of transcriptional

Author Manuscript Author Manuscript Author Manuscript Author Manuscript

or genetic signatures of acinar- and ductal-cell-specific tumors. These signatures could then be correlated with clinical outcomes to examine the role of cellular origin in human PDAC.

Supplementary Material

Refer to Web version on PubMed Central for supplementary material.

Acknowledgements

We thank Nissi Varki (UCSD Cancer Center, Histopathology Core), Fenfen Liu, Nancy Rosenblatt, Sangho Yu, Manbir Sandhu, Christopher Kopp, and Yu Cao for expert technical and statistical assistance. We would also like to thank Andrew Lowy for advice and members of the Sander and Kopp laboratories for discussions. We thank Christopher Wright (Vanderbilt University; *Ptf1a*^{CreER} mice), David Tuveson (Cold Spring Harbor Laboratory; *Kras*$^{LSL\text{-}G12D}$ mice), Chrissa Kioussi (Oregon State University; anti-GFP antibody) and NovoNordisk (anti-Sox9 antibody) for their contribution of mice or reagents. This work was supported by NIH-R01DK078803 and R21CA194839 to M.S. and NIH-F32CA136124, Pancreatic Cancer Canada Foundation Innovation Grant, Canadian Foundation for Innovation, Pancreas Centre BC, and CIHR Open Operating and New Investigator grants to J.L.K, and a University of British Columbia Faculty of Medicine Graduate Award to A.L. The authors have no conflicts of interest.

Abbreviations used in this paper:

AB	Alcian blue
ABC	Avidin-biotin complex
AC	adenocarcinoma
Acinar:KP^{cKO}	*Ptf1a*^{CreER};*Kras*$^{LSL\text{-}G12D}$;*Trp53*$^{flox/flox}$ mice
BVI	blood vessel invasion
CK19	Cytokeratin 19
CK20	Keratin 20
Cpa1	carboxypeptidase A1
DAB	3-3'-Diaminobenzidine tetrahydrochloride
Duct:KP^{cKO}	*Sox9CreER;Kras*$^{LSL\text{-}G12D}$;*Trp53*$^{flox/flox}$ mice
Duct:R26R^{YFP}	*Sox9CreER;R26R*^{YFP} mice
GFP	green fluorescence protein
H&E	hematoxylin and eosin
IHC	immunohistochemistry
K	*Kras*$^{LSL\text{-}G12D}$ allele
LVI	lymphatic invasion
Met	metastasis
mm	millimeters

Author Manuscript Author Manuscript Author Manuscript Author Manuscript

mPanIN	murine PanIN
Muc5AC	Mucin 5AC
n	sample number
PanINs	pancreatic intraepithelial neoplasia precursor lesions
p^{cKO}	*Trp53^{flox}* allele
PDAC	Pancreatic ductal adenocarcinoma
p.i.	post-injection
PNI	perineural invasion
SEM	standard error of the mean
TBS	Tris buffered saline
YFP	yellow fluorescence protein

REFERENCES

1. Hruban RH, Goggins M, Parsons J, et al. Progression model for pancreatic cancer. Clinical cancer research : an official journal of the American Association for Cancer Research 2000;6(8):2969–72. [PubMed: 10955772]
2. Parsa I, Longnecker DS, Scarpelli DG, et al. Ductal metaplasia of human exocrine pancreas and its association with carcinoma. Cancer Research 1985;45(3):1285–90. [PubMed: 2982487]
3. Sandgren EP, Luetteke NC, Palmiter RD, et al. Overexpression of TGF alpha in transgenic mice: induction of epithelial hyperplasia, pancreatic metaplasia, and carcinoma of the breast. Cell 1990;61(6):1121–35. [PubMed: 1693546]
4. Means AL, Meszoely IM, Suzuki K, et al. Pancreatic epithelial plasticity mediated by acinar cell transdifferentiation and generation of nestin-positive intermediates. Development (Cambridge, England) 2005;132(16):3767–76. [PubMed: 16020518]
5. Strobel O, Dor Y, Alsina J, et al. In Vivo Lineage Tracing Defines the Role of Acinar-to-Ductal Transdifferentiation in Inflammatory Ductal Metaplasia. Gastroenterology 2007;133(6):1999–2009. [PubMed: 18054571]
6. Bailey JM, Hendley AM, Lafaro KJ, et al. p53 mutations cooperate with oncogenic Kras to promote adenocarcinoma from pancreatic ductal cells. Oncogene 2016;35(32):4282–8. [PubMed: 26592447]
7. Guerra C, Schuhmacher AJ, Cañamero M, et al. Chronic pancreatitis is essential for induction of pancreatic ductal adenocarcinoma by K-Ras oncogenes in adult mice. Cancer Cell 2007;11(3):291–302. [PubMed: 17349585]
8. Habbe N, Shi G, Meguid RA, et al. Spontaneous induction of murine pancreatic intraepithelial neoplasia (mPanIN) by acinar cell targeting of oncogenic Kras in adult mice. Proceedings of the National Academy of Sciences 2008;105(48):18913–18.
9. Ji B, Tsou L, Wang H, et al. Ras Activity Levels Control the Development of Pancreatic Diseases. Gastroenterology 2009;137(3):1072–82.e6. [PubMed: 19501586]
10. Kopp JL, von Figura G, Mayes E, et al. Identification of Sox9-Dependent Acinar-to-Ductal Reprogramming as the Principal Mechanism for Initiation of Pancreatic Ductal Adenocarcinoma. Cancer Cell 2012;22(6):737–50. [PubMed: 23201164]
11. De La OJP, Emerson LL, Goodman JL, et al. Notch and Kras reprogram pancreatic acinar cells to ductal intraepithelial neoplasia. Proceedings of the National Academy of Sciences 2008;105(48):18907–12.

Author Manuscript Author Manuscript Author Manuscript Author Manuscript

12. Ray KC, Bell KM, Yan J, et al. Epithelial tissues have varying degrees of susceptibility to Kras(G12D)-initiated tumorigenesis in a mouse model. PLoS ONE 2011;6(2):e16786. [PubMed: 21311774]
13. Ferreira RMM, Sancho R, Messal HA, et al. Duct- and Acinar-Derived Pancreatic Ductal Adenocarcinomas Show Distinct Tumor Progression and Marker Expression. Cell Rep 2017;21(4):966–78. [PubMed: 29069604]
14. von Figura G, Fukuda A, Roy N, et al. The chromatin regulator Brg1 suppresses formation of intraductal papillary mucinous neoplasm and pancreatic ductal adenocarcinoma. Nat Cell Biol 2014;16(3):255–67. [PubMed: 24561622]
15. Bailey P, Chang DK, Nones K, et al. Genomic analyses identify molecular subtypes of pancreatic cancer. Nature 2016;531(7592):47–52. [PubMed: 26909576]
16. Morris JP, Cano DA, Sekine S, et al. Beta-catenin blocks Kras-dependent reprogramming of acini into pancreatic cancer precursor lesions in mice. The Journal of clinical investigation 2010;120(2):508–20. [PubMed: 20071774]
17. Seymour PA, Freude KK, Dubois CL, et al. A dosage-dependent requirement for Sox9 in pancreatic endocrine cell formation. Dev Biol 2008;323(1):19–30. [PubMed: 18723011]
18. Kopp JL, Dubois CL, Schaffer AE, et al. Sox9+ ductal cells are multipotent progenitors throughout development but do not produce new endocrine cells in the normal or injured adult pancreas. Development (Cambridge, England) 2011;138(4):653–65. [PubMed: 21266405]
19. Hruban RH, van Mansfeld AD, Offerhaus GJ, et al. K-ras oncogene activation in adenocarcinoma of the human pancreas. A study of 82 carcinomas using a combination of mutant-enriched polymerase chain reaction analysis and allele-specific oligonucleotide hybridization. Am J Pathol 1993;143(2):545–54. [PubMed: 8342602]
20. Scarpa A, Capelli P, Mukai K, et al. Pancreatic adenocarcinomas frequently show p53 gene mutations. Am J Pathol 1993;142(5):1534–43. [PubMed: 8494051]
21. Tuveson DA, Shaw AT, Willis NA, et al. Endogenous oncogenic K-ras(G12D) stimulates proliferation and widespread neoplastic and developmental defects. Cancer Cell 2004;5(4):375–87. [PubMed: 15093544]
22. Marino S, Vooijs M, van Der Gulden H, et al. Induction of medulloblastomas in p53-null mutant mice by somatic inactivation of Rb in the external granular layer cells of the cerebellum. Genes & development 2000;14(8):994–1004. [PubMed: 10783170]
23. Srinivas S, Watanabe T, Lin CS, et al. Cre reporter strains produced by targeted insertion of EYFP and ECFP into the ROSA26 locus. BMC Dev Biol 2001;1(4):4. [PubMed: 11299042]
24. Font-Burgada J, Shalapour S, Ramaswamy S, et al. Hybrid Periportal Hepatocytes Regenerate the Injured Liver without Giving Rise to Cancer. Cell 2015;162(4):766–79. [PubMed: 26276631]
25. Pan FC, Bankaitis ED, Boyer D, et al. Spatiotemporal patterns of multipotentiality in Ptf1a-expressing cells during pancreas organogenesis and injury-induced facultative restoration. Development 2013;140(4):751–64. [PubMed: 23325761]
26. Kim GE, Bae HI, Park HU, et al. Aberrant expression of MUC5AC and MUC6 gastric mucins and sialyl Tn antigen in intraepithelial neoplasms of the pancreas. Gastroenterology 2002;123(4):1052–60. [PubMed: 12360467]
27. Moffitt RA, Marayati R, Flate EL, et al. Virtual microdissection identifies distinct tumor- and stroma-specific subtypes of pancreatic ductal adenocarcinoma. Nat Genet 2015;47(10):1168–78. [PubMed: 26343385]
28. DiGiuseppe JA, Hruban RH, Goodman SN, et al. Overexpression of p53 protein in adenocarcinoma of the pancreas. Am J Clin Pathol 1994;101(6):684–8. [PubMed: 8209852]
29. Yamano M, Fujii H, Takagaki T, et al. Genetic progression and divergence in pancreatic carcinoma. Am J Pathol 2000;156(6):2123–33. [PubMed: 10854233]
30. von Figura G, Morris JPt, Wright CV, et al. Nr5a2 maintains acinar cell differentiation and constrains oncogenic Kras-mediated pancreatic neoplastic initiation. Gut 2014;63(4):656–64. [PubMed: 23645620]
31. Flandez M, Cendrowski J, Canamero M, et al. Nr5a2 heterozygosity sensitises to, and cooperates with, inflammation in KRas(G12V)-driven pancreatic tumourigenesis. Gut 2014;63(4):647–55. [PubMed: 23598351]

Author Manuscript Author Manuscript Author Manuscript Author Manuscript

32. Krah NM, De La OJ, Swift GH, et al. The acinar differentiation determinant PTF1A inhibits initiation of pancreatic ductal adenocarcinoma. Elife 2015;4.
33. Shi G, DiRenzo D, Qu C, et al. Maintenance of acinar cell organization is critical to preventing Kras-induced acinar-ductal metaplasia. Oncogene 2012.
34. Shi G, Zhu L, Sun Y, et al. Loss of the acinar-restricted transcription factor Mist1 accelerates Kras-induced pancreatic intraepithelial neoplasia. Gastroenterology 2009;136(4):1368–78. [PubMed: 19249398]
35. Collins MA, Bednar F, Zhang Y, et al. Oncogenic Kras is required for both the initiation and maintenance of pancreatic cancer in mice. The Journal of clinical investigation 2012;122(2):639–53. [PubMed: 22232209]
36. Roy N, Malik S, Villanueva KE, et al. Brg1 promotes both tumor-suppressive and oncogenic activities at distinct stages of pancreatic cancer formation. Genes & development 2015;29(6):658–71. [PubMed: 25792600]
37. Guerra C, Collado M, Navas C, et al. Pancreatitis-induced inflammation contributes to pancreatic cancer by inhibiting oncogene-induced senescence. Cancer Cell 2011;19(6):728–39. [PubMed: 21665147]
38. Hingorani SR, Wang L, Multani AS, et al. Trp53R172H and KrasG12D cooperate to promote chromosomal instability and widely metastatic pancreatic ductal adenocarcinoma in mice. Cancer Cell 2005;7(5):469–83. [PubMed: 15894267]
39. Aguirre AJ, Bardeesy N, Sinha M, et al. Activated Kras and Ink4a/Arf deficiency cooperate to produce metastatic pancreatic ductal adenocarcinoma. Genes & development 2003;17(24):3112–26. [PubMed: 14681207]
40. Bardeesy N, Aguirre AJ, Chu GC, et al. Both p16(Ink4a) and the p19(Arf)-p53 pathway constrain progression of pancreatic adenocarcinoma in the mouse. Proceedings of the National Academy of Sciences of the United States of America 2006;103(15):5947–52. [PubMed: 16585505]
41. Pérez-Mancera PA, Guerra C, Barbacid M, et al. What We Have Learned About Pancreatic Cancer from Mouse Models. YGAST 2012:1–39.
42. Hassid BG, Lucas AL, Salomao M, et al. Absence of pancreatic intraepithelial neoplasia predicts poor survival after resection of pancreatic cancer. Pancreas 2014;43(7):1073–77. [PubMed: 24987871]
43. Oda Y, Aishima S, Morimatsu K, et al. Pancreatic intraepithelial neoplasia in the background of invasive ductal carcinoma of the pancreas as a prognostic factor. Histopathology 2014;65(3):389–97. [PubMed: 24931343]
44. Miyazaki T, Ohishi Y, Miyasaka Y, et al. Molecular Characteristics of Pancreatic Ductal Adenocarcinomas with High-Grade Pancreatic Intraepithelial Neoplasia (PanIN) Are Different from Those without High-Grade PanIN. Pathobiology 2017;84(4):192–201. [PubMed: 28291966]

Author Manuscript Author Manuscript Author Manuscript Author Manuscript

SIGNIFICANCE OF THIS STUDY

What is already known about this subject:

- Oncogenic $Kras^{G12D}$ mutations are hypothesized to initiate preneoplastic pancreatic lesions, called pancreatic intraepithelial neoplasia (PanIN), which subsequently acquire other genetic alterations, like *Trp53* loss, to form pancreatic ductal adenocarcinoma (PDAC).
- $Kras^{G12D}$ expression in acinar cells induces numerous low-grade murine PanIN (mPanIN) lesions, while few are induced from $Kras^{G12D}$-expressing ductal cells.
- $Kras^{G12D}$-expressing acinar cells can form PDAC in the presence of heterozygous mutations in *Trp53*, while homozygous mutations in *Trp53* are needed for $Kras^{G12D}$ to transform ductal cells.

What are the new findings:

- PDAC forms faster from ductal than acinar cells when the same mutations and conditions are present, demonstrating that cell of origin alone can affect tumor development.
- High-grade mPanIN are quickly induced from both $Kras^{G12D}$-expressing ductal and acinar cells lacking *Trp53*, however, ductal-cell-derived mPanIN3 become invasive faster than acinar-cell-derived mPanIN3.
- Acinar-cell-mediated tumorigenesis is associated with low-grade mPanINs and characteristics of low-grade mPanIN are found in acinar cell-derived PDAC, suggesting that cell of origin can affect tumor phenotype.

How might it impact on clinical practice in the foreseeable future?

- Acinar and ductal cells are capable of initiating tumorigenesis in mice. These novel mouse models may be helpful in identifying the cellular origin of human disease in the future.
- These studies demonstrate that cell of origin alone could impact the development and phenotype of PDAC.
- Preclinical animal model studies should consider the important effects of cellular origin on the phenotype of PDAC and its response to treatment, and disease outcomes.

Author Manuscript Author Manuscript Author Manuscript Author Manuscript

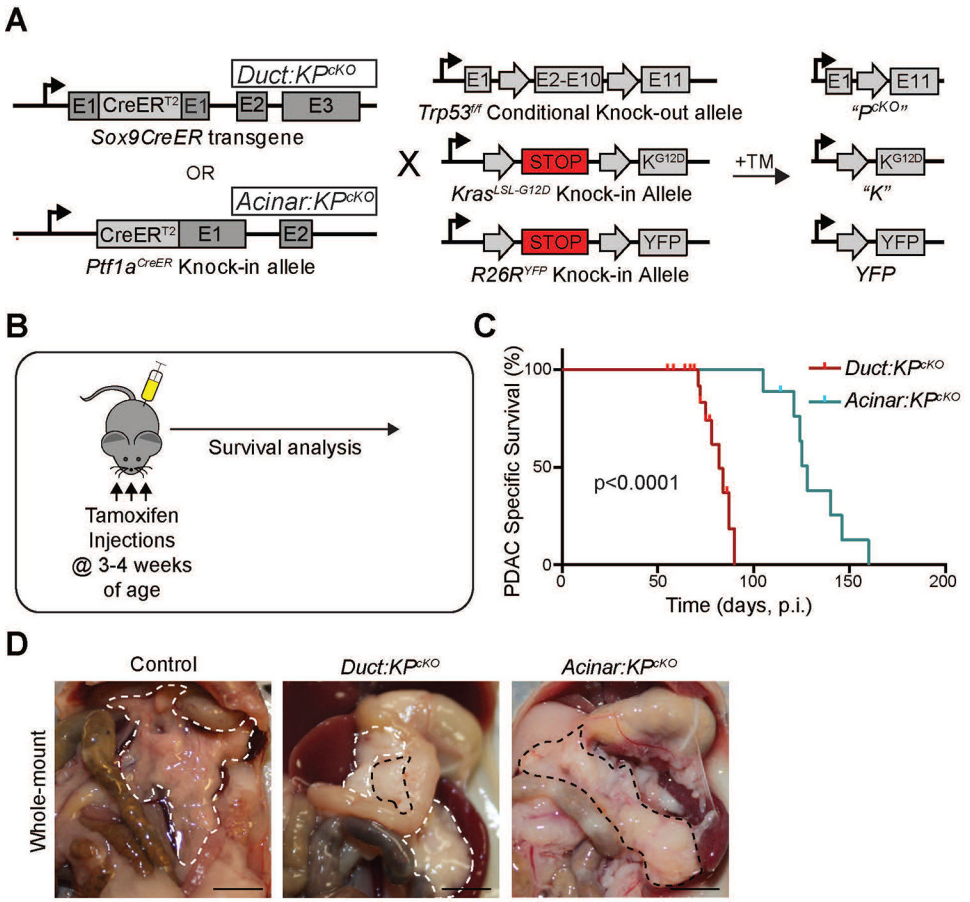

Figure 1. Kras^{G12D}-expressing ductal cells form tumors earlier than acinar cells in the absence of *Trp53*.

(A) Schematic of the alleles in the *Sox9CreER;Kras$^{LSL-G12D}$;Trp53$^{flox/flox}$;R26R^{YFP}* (*Duct:KP^{cKO}*) and *Ptf1a^{CreER};Kras$^{LSL-G12D}$;Trp53$^{flox/flox}$;R26R^{YFP}* (*Acinar:KP^{cKO}*) mouse models used in this study. Tamoxifen (TM) injection induces Cre-mediated DNA recombination and results in expression of oncogenic Kras^{G12D} from the *Kras$^{LSL-G12D}$* ("*K*") allele and the YFP lineage label from the *R26R^{YFP}* allele. In addition, TM injection induces the deletion of exons 2–10 from the *Trp53^{flox}* ("*P^{cKO}*") allele and loss of p53 expression. (B) *Duct:KP^{cKO}* (n=19) and *Acinar:KP^{cKO}* (n=9) mice were injected three times on alternating days with TM beginning at three-four weeks of age. The mice were monitored until they reached their humane endpoint to determine survival duration. (C) The median disease specific survival of *Duct:KP^{cKO}* and *Acinar:KP^{cKO}* mice (82 vs. 128 days, p<0.0001). Mice euthanized due to non-pancreatic reasons were censored (hash marks). (D) Representative gross anatomical photographs of the mouse abdomen from *Sox9CreER;Trp53$^{flox/flox}$;R26R^{YFP}* (Control), *Duct:KP^{cKO}*, and *Acinar:KP^{cKO}* mice. White or black dashed lines outline either normal parenchyma or tumors, respectively. p.i., post tamoxifen injection. Scale bars: 5 mm.

Author Manuscript Author Manuscript Author Manuscript Author Manuscript

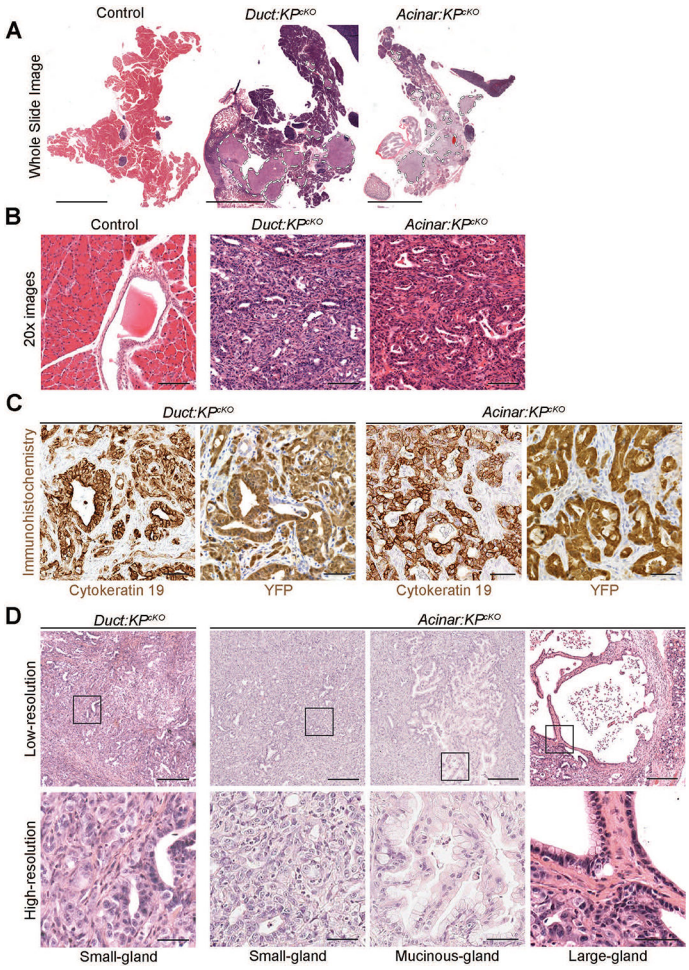

Figure 2. *Duct:KP^{cKO}* and *Acinar:KP^{cKO}* mice develop PDAC.

Representative whole section (A) and high-magnification (B) images of *Sox9CreER;Trp53$^{flox/flox}$;R26R^{YFP}* (Control), *Duct:KP^{cKO}*, and *Acinar:KP^{cKO}* pancreata stained with hematoxylin and eosin (H&E). Tumors are outlined with dashed lines in (A). (B) H&E staining shows that PDAC in *Duct:KP^{cKO}* and *Acinar:KP^{cKO}* mice are predominantly moderately-to-poorly differentiated. (C) Immunohistochemistry for ductal cell marker, Cytokeratin 19, and the YFP lineage marker demonstrates that duct-like tumors in *Duct:KP^{cKO}* and *Acinar:KP^{cKO}* mice arise from ductal and acinar cells, respectively. (D) Low- (top row) and high-(bottom row) magnification images of H&E staining of the different histological tumor phenotypes observed in *Duct:KP^{cKO}* and *Acinar:KP^{cKO}* mice. The small-gland phenotype was observed in both mouse models. The mucinous-gland and large-gland phenotypes were found more often in *Acinar:KP^{cKO}* mice and rarely, if ever, in *Duct:KP^{cKO}* mice. Scale bars: 5 mm (A), 100 μm (B), 200 μm (D, top), and 50 μm (D, bottom and C).

Author Manuscript Author Manuscript Author Manuscript Author Manuscript

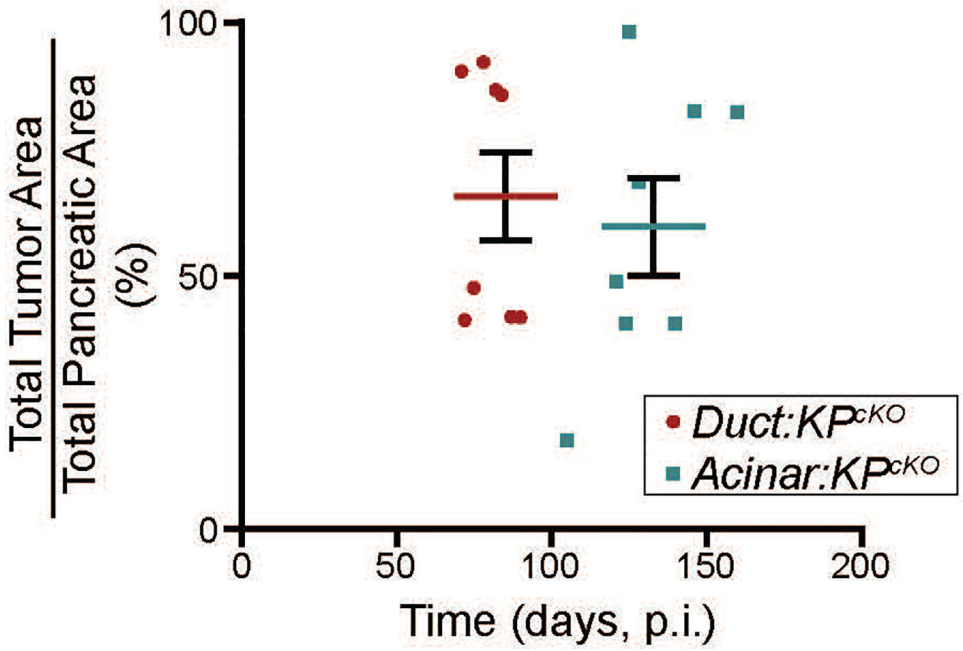

Figure 3. Tumor burden in *Duct:KP^{cKO}* and *Acinar:KP^{cKO}* mice at humane endpoint is similar, but reaches the peak amount earlier in *Duct:KP^{cKO}* mice.

Quantification of the pancreatic area displaced by tumor area in individual *Duct:KP^{cKO}* (n=8) and *Acinar:KP^{cKO}* (n=8) mice at their humane endpoint (66.0% ± 8.7% vs. 60.0% ± 9.7%, p=0.4) plotted against time post tamoxifen injection (p.i.). All values shown as mean ± SEM.

Author Manuscript Author Manuscript Author Manuscript Author Manuscript

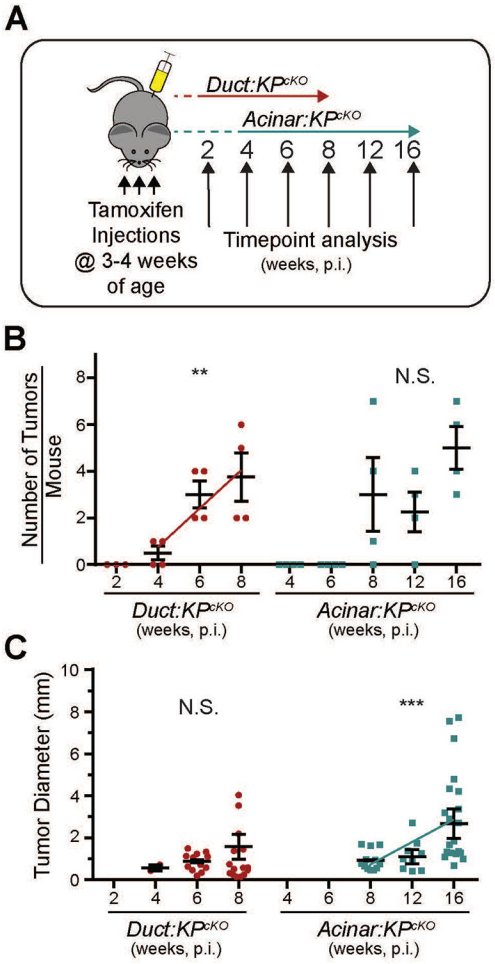

Figure 4. Tumors arise earlier in *Duct:KP^{cKO}* compared to *Acinar:KP^{cKO}* mice.

(A) Schematic describing the experimental design. *Duct:KP^{cKO}* and *Acinar:KP^{cKO}* mice (n=4) were injected with tamoxifen at 3–4 weeks of age and euthanized at 2, 4, 6 and 8 weeks post injection (p.i.) or 4, 6, 8, 12, and 16 weeks p.i. for *Duct:KP^{cKO}* or *Acinar:KP^{cKO}* mice, respectively. Quantification of the number of tumors present (B) and the cross-sectional diameter of each tumor (C) in these *Duct:KP^{cKO}* and *Acinar:KP^{cKO}* mice revealed that tumors initiated earlier from ductal compared to acinar cells. Trend lines in the graph indicate significant correlations between time and tumor number (B) or size (C). All values shown as mean ± SEM. mm, milimeters. **, $p<0.01$ and ***, $p<0.001$.

Author Manuscript Author Manuscript Author Manuscript Author Manuscript

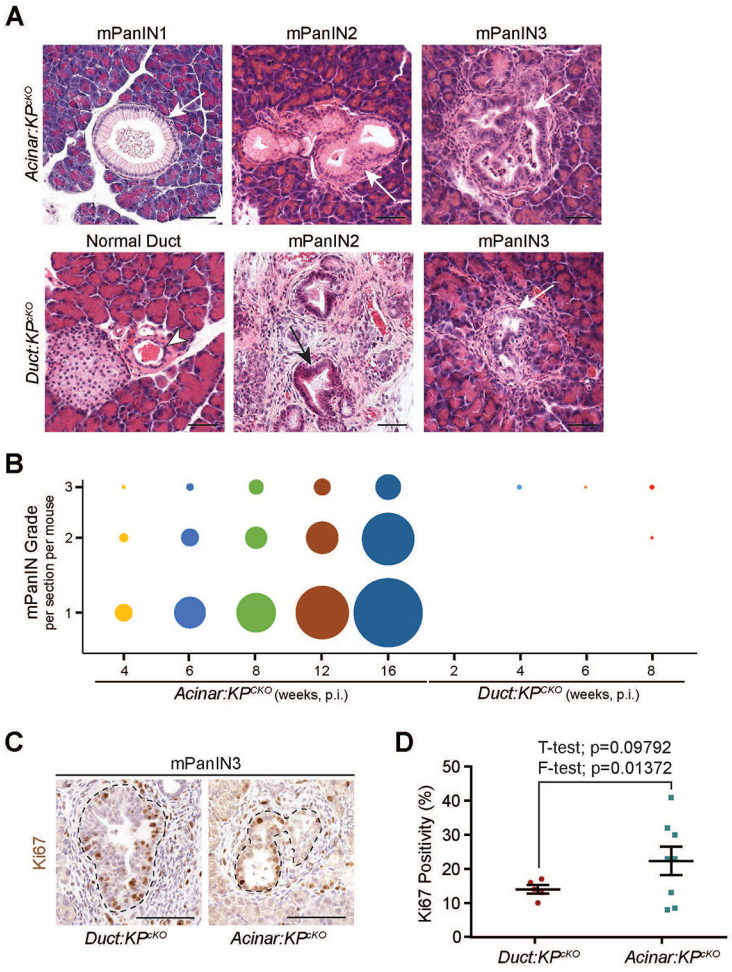

Figure 5. Kras^{G12D} expression and loss of p53 induces a spectrum of mPanIN lesions from acinar cells, but predominately high-grade mPanIN from ductal cells.

(A) Representative images of hematoxylin and eosin stained normal duct (arrowhead), mPanIN1, 2 or 3 lesions (arrows) found in *Acinar:KP^{cKO}* and *Duct:KP^{cKO}* mice. No mPanIN1 lesions were observed in *Duct:KP^{cKO}* mice. (B) Quantification of the average number of mPanIN lesions of each grade present per section per mouse at the indicated time points post tamoxifen injection (p.i.) in *Duct:KP^{cKO}* and *Acinar:KP^{cKO}* mice. The number of mPanIN1 in the *Acinar:KP^{cKO}* line at 16 weeks post injection was set to 1 and the other circles represent the fraction of mPanIN present per time point or grade in *Duct:KP^{cKO}* and *Acinar:KP^{cKO}* mice relative to that sample. Immunohistochemistry for proliferation marker Ki67 (C) and quantification of the Ki67^{+} cells per mPanIN3 (D) in *Duct:KP^{cKO}* and *Acinar:KP^{cKO}* mice. Scale bar: 50 μm (A), 100 μm (C).

Author Manuscript Author Manuscript Author Manuscript Author Manuscript

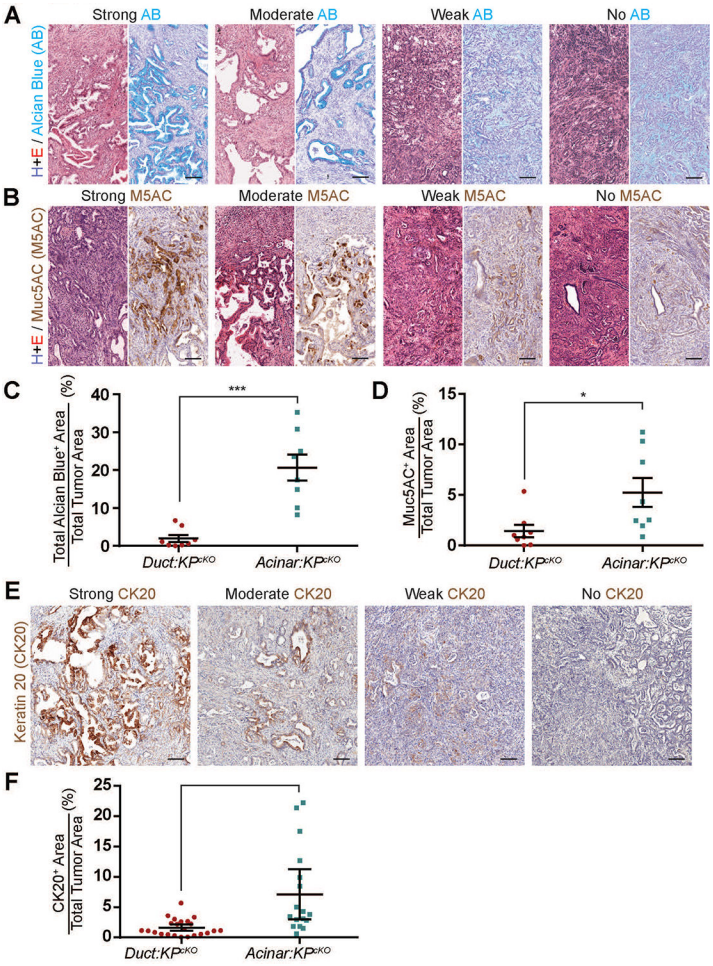

Figure 6. Glandular areas containing gastric mucin expression are more prevalent in tumors from *Acinar:KP^{cKO}* compared to *Duct:KP^{cKO}* mice.

Representative images of tumor areas from *Duct:KP^{cKO}* and *Acinar:KP^{cKO}* mice stained with hematoxylin and eosin (H&E)(A-B, left panels) or Alcian blue (AB) (A, right panels) or Mucin 5AC (Muc5AC or M5AC) (B, right panels). Light Alcian blue staining in the stroma or Muc5AC staining in blood vessels or blood cells was classified as negative. The Muc5AC staining is likely an artifact of the anti-mouse secondary antibody. Quantification of the percent of AB (C) or Muc5AC (D) positive tumor area in *Duct:KP^{cKO}* and *Acinar:KP^{cKO}* mice (AB: 20.7% vs 2%, respectively, $p<0.001$ (***) and Muc5AC: 5.3% vs. 1.4%, respectively, $p<0.05$ (*)). (E) Representative images of tumor areas from *Duct:KP^{cKO}* and *Acinar:KP^{cKO}* mice stained with Cytokeratin 20 (CK20). Quantification of the percent of CK20 positive tumor area in *Duct:KP^{cKO}* and *Acinar:KP^{cKO}* mice ($p<0.0001$ (****)). All values shown as mean ± SEM. Scale bar: 100 μm (A-B).

Author Manuscript Author Manuscript Author Manuscript Author Manuscript

Gut. Author manuscript; available in PMC 2024 November 01.

Table 1.

Characterization of *Duct:KP^{cKO}* and *Acinar:KP^{cKO}* mice.

Genotype	Mouse ID	Time (days, p.i.)	Jaundice	Liver Lesion	Distant met		Local invasion			Ascites	Cytokeratin 19 IHC	Histological type		Tumor Area (% of total pancreatic area)
					Diaphragm	Peritoneum	Spleen	Duodenum	PNI/ LVI/ BVI			Large-gland	Mucinous-gland	
Duct:KP^{cKO}	144	71			X	X	X	X	X		+++	0/7	2/7	90
	107	72	X	X				X			+++	0/4	1/4	41
	469	75	X	X				X		B	+++	0/10	0/10	48
	499	78		X					X	B	+++	0/4	0/4	92
	433	82		X				X			+++	0/8	0/8	87
	479	84		X	X	X			X	B	+++	0/5	0/5	86
	477	87									+++	0/5	0/5	42
	369	90						X			+++	0/5	0/4	42
Acinar:KP^{cKO}	97	105	X								+++	3/5	0/5	18
	23	121						X			+++	0/5	1/5	49
	94	124								C	+++	3/8	0/8	41
	27	125							X		+++	1/3	1/3	98
	100	128	X								+++	3/5	0/5	69
	52	140	X					X	X		+++	1/5	0/5	41
	92	146					X		X	B	+++	0/4	2/4	82
	33	160					X	X	X	C	+++	0/6	4/6	82

ID, mouse identification number; p.i., post injection; met, metastasis; PNI, perineural invasion; LVI, lymphatic invasion; BVI, blood vessel invasion; IHC, immunohistochemistry; X, characteristic present; B, hemorrhagic ascites fluid; C, Clear ascites fluid; and +++, strong positive IHC positivity.